1,3-Dipolar Cycloadditions to Baylis–Hillman Adducts: Rationale for the Observed Diastereoselectivity

Rita Annunziata,* Maurizio Benaglia, Mauro Cinquini, Franco Cozzi, and Laura Raimondi*

Centro CNR and Dipartimento di Chimica Organica e Industriale, via Golgi 19, 20133 Milano, Italy

Received September 26, 1994 (Revised Manuscript Received April 18, 1995®)

Diazomethane and benzonitrile oxide cycloadditions were performed on Baylis–Hillman adducts derived from methyl acrylate and aldehydes (β'-alkoxy-α,β-unsaturated esters). The reactions proceed in good chemical yields, and their stereochemical outcome can be explained by the "inside alkoxy effect" theory. In the case of diazomethane cycloadditions, however, electrostatic factors play a reduced role in comparison to the corresponding nitrile oxide reactions, while steric effects are of major importance in governing the stereoselectivity. This different behavior of the two 1,3-dipoles finds a rationale in the analysis of the atomic charges as calculated at the RHF/3-21G level of theory for the transition structure of these reactions.

Introduction

1,3-Dipolar cycloadditions to alkenes are widely used in organic synthesis due to the generally high stereoselectivity of these reactions and to the synthetic versatility of the corresponding heterocyclic products.[1] The origin of the stereoselectivity in these processes has been deeply investigated, and useful theories, such as the "inside alkoxy effect",[2] were formulated; this rationale was subsequently extended from the particular case of nitrile oxide cycloadditions to a variety of electrophilic addition reactions to chiral alkenes.[3]

The inside alkoxy theory, based upon *ab initio* calculations, states that the preferred conformation for the transition state of the reaction between a nitrile oxide and a chiral allyl ether, leading to a 5-substituted 4,5-dihydroisoxazole, is the one featuring the allylic oxygen in the *inside* position. The *outside* position is strongly destabilized by the electrostatic repulsion between the allylic and the nitrile oxide oxygens, while the *anti* one is preferentially occupied by an electron donating group (*e.g.* an alkyl group; Figure 1).[2]

The nature of the allylic oxygen plays an important role in determining the level of stereoselection, the best results being achieved with a basic, hard, and not hydrogen bearing oxygen. For instance, the reaction of allylic ethers is *anti* selective, while that of the corresponding esters is generally stereorandom.[1,2] An ethereal oxygen can be efficiently replaced by any heteroatom with similar characteristics, *e.g.* the nitrogen of a tertiary amine.[1]

The conformational preferences for the transition structure of these reactions were recently re-examined by performing *ab initio* calculations at higher levels of theory.[4] The effect of the electrostatic interactions was found to overwhelm more subtle stereoelectronic effects (such as orbital interactions) that were postulated to account for the energy difference between the *inside* and the *anti* positions for the ethereal oxygen (Figure 1).[2] Thus, the *inside* position is favored by at least 0.7 kcal/mol over the *anti* one at the RHF/3-21G level,[2,4] but this difference drops to 0.2 kcal/mol when electronic correlation is taken into account (MP2/6-31G*//RHF/3-21G).[4] The *outside* region, on the other hand, stays strongly destabilized at all levels of theory because of the strong electrostatic repulsion due to the negatively charged oxygen of the incoming nitrile oxide.

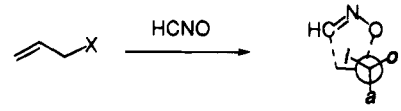

	X = Me[a]	X = OMe[a]	X = OMe[b]
inside	1.1	0.0	0.0
anti	0.0	0.7	0.2
outside	0.6	2.9	2.0

a) ref. 2a. RHF/3-21G calculations.
b) ref. 4. MP2/6-31G*//3-21G calculations.

Figure 1. *Ab initio* energy values (kcal/mol) for nitrile oxide cycloadditions to alkenes.

A striking example of a stereochemical outcome of a nitrile oxide reaction that can find a rationale only when electrostatic interactions are considered came recently from a paper by Kim and co-workers:[5] methyl nitrile oxide reacts with three different camphorsultames attacking preferentially the more hindered diastereoface of the alkenes. This behavior was ascribed to the electrostatic repulsion between the incoming nitrile oxide oxygen and the axial oxygen of the sulfone, which effectively disfavors the attack on the less hindered diastereoface.

To evaluate the effect of electrostatic factors in affecting the stereoselectivity of 1,3-dipolar cycloaddition reactions, the atomic charges in the transition structure for the cycloaddition of five different 1,3-dipoles to ethylene were calculated (Figure 2).[6] If the sense of stereoselectivity is determined mainly by the nature of the substit-

® Abstract published in *Advance ACS Abstracts,* June 15, 1995.

(1) (a) Annunziata, R.; Cinquini, M.; Cozzi, F.; Raimondi, L. *Gazz. Chim. Ital.* **1989**, *119*, 253. (b) Kamimura, A. *J. Synth. Org. Chem. Jpn.* **1992**, 808.

(2) (a) Houk, K. N.; Moses, S. R.; Wu, Y.-D.; Rondan, N. G.; Jäger, V.; Schohe, R.; Fronczek, F. R. *J. Am. Chem. Soc.* **1984**, *106*, 3880. (b) Houk, K. N.; Duh, H.-Y.; Wu, Y.-D.; Moses, S. R. *J. Am. Chem. Soc.* **1986**, *108*, 2754.

(3) Houk, K. N.; Paddon-Row, M. N.; Rondan, N. G.; Wu, Y.-D.; Brown, F. K.; Spellmeyer, D. C.; Metz, J. T.; Li, Y.; Loncharich, R. J. *Science* **1986**, *231*, 1108.

(4) Brown, F. K.; Raimondi, L.; Wu, Y.-D.; Houk, K. N. *Tetrahedron Lett.* **1992**, *33*, 4409.

(5) Kim, K. S.; Kim, B. H.; Park, W. M.; Cho, S. J.; Mhin, B. J. *J. Am. Chem. Soc.* **1993**, *115*, 7472.

0022-3263/95/1960-4697$09.00/0

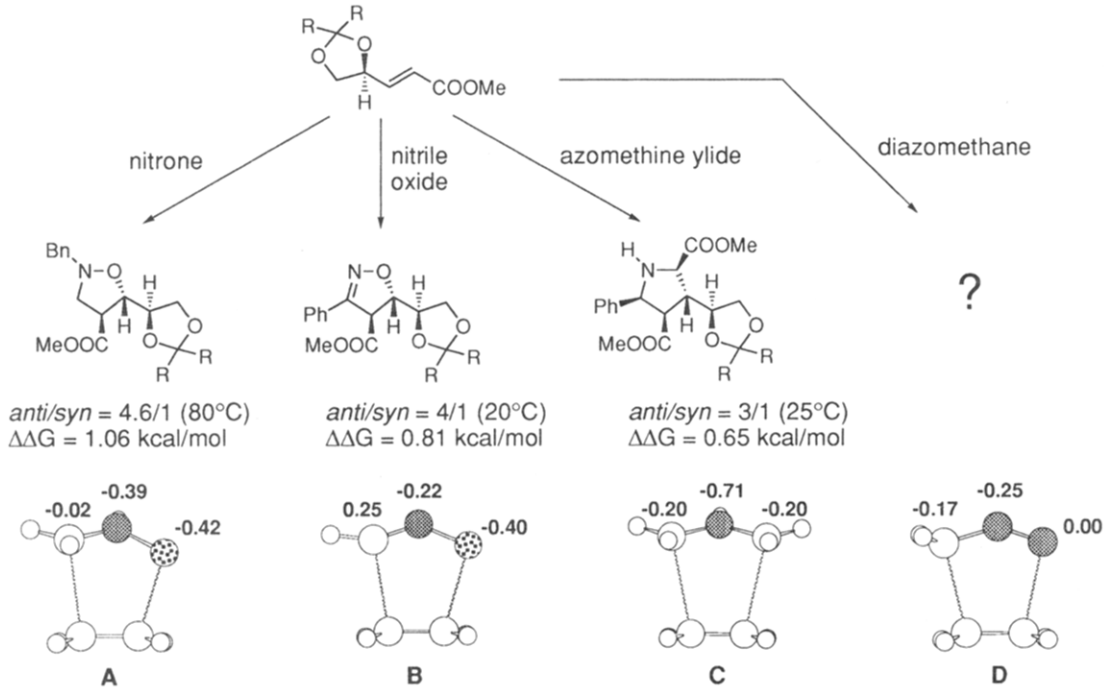

Figure 2. Atomic charges on transition structures compared with the differences in stereoselectivity between various 1,3-dipoles (ref 6). Only *anti* (major) isomers are shown for simplicity.

uents at the allylic stereocenter of the alkene, the amount of stereoselectivity is determined by the nature of the 1,3-dipole; in particular, it seems to correlate with the amount of negative charge present on the terminal atom of the dipole moiety. For instance, the charge on the terminal oxygen of a nitrone is more negative than that of a nitrile oxide—and generally nitrone cycloadditions are more selective.[1,6]

Diazomethane (**D**) and nitrile oxide (**B**) transition structures are planar and possess C_s symmetry, the plane being the one containing the forming five-membered ring (Figure 2); thus, they can be directly compared, all other factors (*e.g.* steric interactions) being probably similar. From a comparison of the atomic charges on the terminal heteroatom in the nitrile oxide and diazomethane transition structures, it can be seen that in the last case the terminal nitrogen features the lowest negative charge. On this basis, three hypotheses can be advanced: (i) diazomethane reactions should be less stereoselective than those of nitrile oxide and nitrone; (ii) the sense and extent of stereoselection in diazomethane cycloadditions should be determined mainly by steric effects; (iii) the stereoselectivity of these reactions should not be strongly sensitive to the nature of the heteroatom in the allylic position.[8] The present experimental study was undertaken to confirm these predictions.

Results and Discussions

Some major problems are unavoidable when diazomethane reactions are performed. The high volatility of this product, its toxicity, and the risks of explosions impose caution in the choice of the reaction conditions, which must be as mild as possible. On the other hand, this dipole exhibits a low reactivity toward unactivated alkenes: various attempts to react it with a terminal, unactivated olefin such as 3-(benzyloxy)-1-butene were unsuccessful. Activated alkenes were therefore needed. Unfortunately, diazomethane cycloadditions on γ-alkoxy-α,β-unsaturated esters (as the one shown in Figure 2) gave selectively the undesired regioisomer, with the nitrogen attacking the α-carbon of the conjugated alkene. Moreover, the resulting cycloadducts are quite unstable products; thus, we turned our attention to the so-called Baylis–Hillman adducts **1**–**12**, shown in Scheme 1.

The synthesis of the allylic alcohols **1**–**4** was accomplished by stirring a mixture of the reactants with a catalytic amount of DABCO at room temperature for 7–10 days.[7] Treatment of **1**–**4** with TBDMSCl in DMF in the presence of imidazole afforded the *O*-silyl derivatives **5**–**8**. To synthesize the acetoxy derivatives **9**–**12**, treatment with acetyl chloride of **1**–**4** was essential; other reagents (such as Ac_2O) led to the formation of rearranged products.

Benzonitrile Oxide Cycloadditions. Benzonitrile oxide was shown to react with alkene **1** to give predominantly the inside alkoxy product with good stereoselectivity.[8] However, no systematic study was ever undertaken to assess the behavior of the Baylis–Hillman adducts in their reaction with nitrile oxides. Since the purpose of this work was to compare diazomethane and

(6) Annunziata, R.; Benaglia, M.; Cinquini, M.; Raimondi, L. *Tetrahedron* **1993**, *49*, 8629.

(7) (a) Hoffmann, H. M. R.; Rabe, J. *Angew. Chem., Int. Ed. Engl.* **1983**, *22*, 795. (b) Hoffmann, H. M. R.; Rabe, J. *J. Org. Chem.* **1985**, *50*, 3849. (c) Drewes, S. E.; Hoole, R. F. A. *Synth. Commun.* **1985**, *15*, 1067. (d) Ameer, F.; Drewes, S. E.; Freese, S.; Kaye, P. T. *Synth. Commun.* **1988**, *18*, 495.

(8) Recently, nitrile oxide cycloadditions were performed on some Baylis–Hillman adducts: Kanemasa, S.; Kobayashi, S. *Bull. Chem. Soc. Jpn.* **1993**, *66*, 2685. These authors define the inside alkoxy products as *anti*, but they draw their structures in a different orientation from the one adopted in the present work: those *anti* isomers correspond to our *syn* cycloadducts.

Scheme 1. Synthesis of the Baylis–Hillman Adducts 1–12

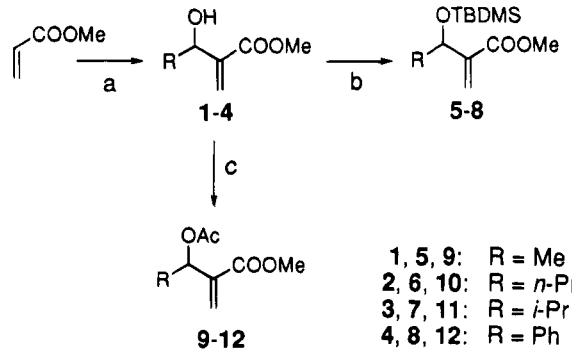

a) RCHO, DABCO; b) TBDMSCl, imidazole, DMF; c) AcCl, Pyridine, CH_2Cl_2.

Table 1. Benzonitrile Oxide Cycloaddition to Baylis–Hillman Adducts 1–12

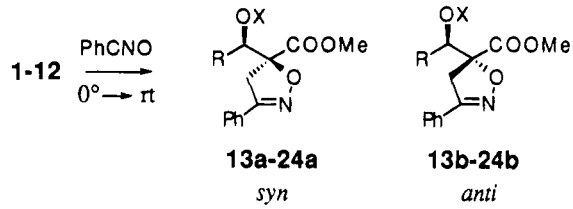

entry	alkene	R	X	product	yield %	a/b
1	**1**	Me	H	**13**	98	74/26
2	**2**	*n*-Pr	H	**14**	93	94/6
3	**3**	*i*-Pr	H	**15**	70	97/3
4	**4**	Ph	H	**16**	51	70/30
5	**5**	Me	TBDMS	**17**	94	86/14
6	**6**	*n*-Pr	TBDMS	**18**	91	87/13
7	**7**	*i*-Pr	TBDMS	**19**	76	88/12
8	**8**	Ph	TBDMS	**20**	70	79/21
9	**9**	Me	Ac	**21**	92	55/45
10	**10**	*n*-Pr	Ac	**22**	96	77/23
11	**11**	*i*-Pr	Ac	**23**	98	90/10
12	**12**	Ph	Ac	**24**	95	52/48

nitrile oxide cycloadditions, we needed to check this point first; thus, benzonitrile oxide was reacted with alkenes **1–12** in Et_2O at 0 °C. The reaction was found to be *syn* stereoselective in all cases, the *syn* product being the one predicted by the inside alkoxy theory.[8] The diastereoisomeric ratios of the resulting cycloadducts **13a,b–24a,b** were determined on the crudes by ^1H NMR spectroscopy and confirmed after purification by flash chromatography.[9] Yields and diastereoisomeric ratios are collected in Table 1; ^1H and ^{13}C selected NMR data are collected in Table 2.

The experimental data clearly show a dependence of the inside alkoxy stereoselectivity on the steric hindrance of the R residue at the allylic stereocenter. Methyl (entries 1, 5, 9) and phenyl groups seem to be the smallest, and the *syn* selectivity is the lowest.[10] The nature of the protecting group at the allylic oxygen is also extremely important to achieve a good *syn* selectivity. As expected, the worst results are obtained with acetyl derivatives **9–12** (entries 9–12).

Attribution of the relative C5–C5′ configuration to 4,5-dihydroisoxazoles **13a,b–24a,b** (see Table 2 for numbering) was an easy task. **13a** and **13b** are known compounds, and their relative configuration was established as *syn* and *anti*, respectively, by NMR experiments.[8] From the NMR data collected in Table 2, a trend is evident in the chemical shift of C4 and C5, which resonate at higher and lower fields, respectively, in the *syn*, **a** isomers. To confirm that all **a** isomers have the same *syn* configuration, a pure sample of **13a** was treated with TBDMSCl in DMF in the presence of imidazole, to afford pure **17a**. **13a** was also converted in **21a** with AcCl and pyridine in CH_2Cl_2 (Scheme 2). Thus, all **a** isomers have a 5–5′ *syn*, relative configuration and all **b** isomers a 5–5′ *anti* relative configuration.

(9) Still, W. C.; Kahn, M.; Mitra, A. *J. Org. Chem.* **1978**, *43*, 2923.
(10) A possible explanation for the low *syn* selectivity of the reactions of the phenyl derivatives **8** and **12** can be found in the flatness of the aromatic ring that can easily assume a nonhindering position.

Table 2. Relevant ^1H and ^{13}C NMR data for products 13–24[a]

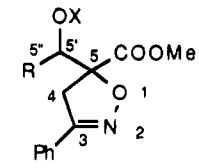

13-24

	^1H			^{13}C				
	4[b]	5′	5″	3	4	5	5′	5″
13a	3.77; 3.57	4.31	1.18	157.1	37.3	92.7	68.4	17.0
13b	3.73; 3.62	4.22	1.27	157.1	40.8	90.0	69.3	17.4
14a	3.76; 3.57	4.11		157.2	37.5	92.4	72.0	33.4
14b	3.74; 3.62	4.04		156.6	41.1	90.8	72.9	33.4
15a	3.83; 3.63	4.01	1.70	157.3	37.3	92.4	76.1	30.0
15b	3.86; 3.67	3.87	1.77	156.8	43.5	91.5	77.0	31.0
16a	3.66	5.35		157.0	37.3	93.0	74.1	130.5
16b	3.76; 3.67	5.25		157.0	40.4	93.0	74.1	130.4
17a	3.79; 3.53	4.37	1.11	156.3	36.4	93.6	69.2	17.3
17b	3.90; 3.50	4.49	1.19	156.6	37.5	91.7	69.5	17.8
18a	3.81; 3.53	4.26		156.8	36.0	92.6	71.8	35.9
18b	3.86; 3.47	4.27		156.7	38.5	91.8	73.9	34.5
19a	3.83; 3.59	4.21	1.58	157.5	36.0	94.0	75.8	30.9
19b	3.59	4.19	1.58	156.0	40.0	92.0	77.6	30.0
20a	3.70	5.30		156.4	36.6	94.2	75.7	130.1
20b	3.88; 3.48	5.36		156.6	38.8	92.0	74.9	129.9
21a	3.80; 3.43	5.45	1.20	155.9	39.1	90.7	70.5	14.8
21b	3.80; 3.44	5.44	1.25	156.2	39.8	89.3	70.5	14.3
22a	3.88; 3.47	5.57		156.2	38.6	90.8	72.8	31.0
22b	3.75; 3.45	5.52		156.2	40.0	89.3	73.4	31.7
23a	3.94; 3.52	5.51	1.87	156.6	37.9	91.1	76.1	29.4
23b	3.70; 3.45	5.40	1.87	156.6	42.0	90.0	76.2	29.6
24a	3.85; 3.50	6.38		156.0	39.5	91.0	75.4	135.0
24b	3.77; 3.55	6.38		156.2	40.0	90.0	74.8	135.5

[a] Chemical shifts in ppm from TMS. [b] AB system.

Scheme 2. Chemical Correlations of Benzonitrile Oxide Cycloaddition Products

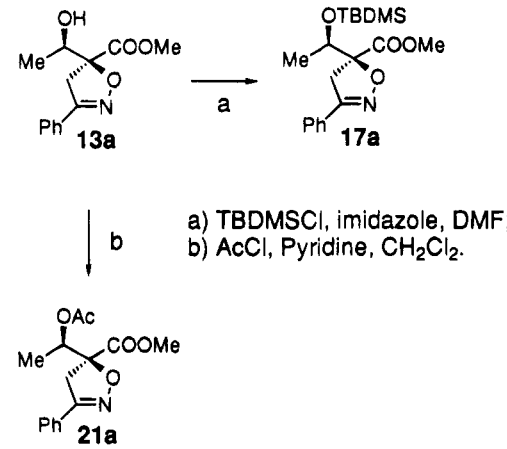

Table 3. Diazomethane Cycloaddition Reaction to Baylis–Hillman Adducts 1–12

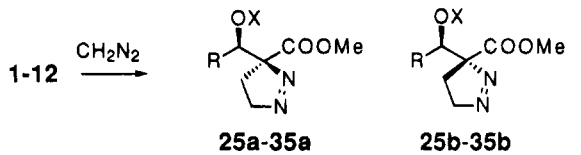

25a-35a *syn* **25b-35b** *anti*

entry	alkene	R	X	product	T (°C)	yield (%)	a/b
1	**5**	Me	TBDMS	**28**	0	98	62/38
2	**6**	*n*-Pr	TBDMS	**29**	0	73	76/24
3	**6**	*n*-Pr	TBDMS	**29**	25	92	76/24
4	**7**	*i*-Pr	TBDMS	**30**	0	67	88/12
5	**7**	*i*-Pr	TBDMS	**30**	25	83	88/12
6	**8**	Ph	TBDMS	**31**	0	88	67/33
7	**9**	Me	Ac	**32**	0	90	58/42
8	**10**	*n*-Pr	Ac	**33**	0	95	74/26
9	**11**	*i*-Pr	Ac	**34**	0	61	73/27
10	**12**	Ph	Ac	**35**	0	90	55/45
11	**1**	Me	H	**25**	0	≥50[a]	85/15
12	**2**	*n*-Pr	H	**26**	0	77	80/20
13	**2**	*n*-Pr	H	**26**	25	48	79/21
14	**3**	*i*-Pr	H	**27**	0	40[b]	≥98/2
15	**4**	Ph	H		*c*	*c*	

[a] The cycloadducts were strongly impure of unidentified decomposition products; flash chromatography procedures did not allow significant purification of the reaction mixture. [b] Only **27a** was detected by NMR spectroscopy, together with decomposition products. [c] Only decomposition products were isolated, independently of the reaction temperature (0, 25 °C).

Diazomethane Cycloadditions. The cycloaddition reaction of adducts **1–12** with diazomethane was accomplished by stirring the alkenes with a 10-fold molar excess of an ethereal solution of diazomethane for 1–2 h: the structures of the resulting 1-pyrazolines **25a,b–35a,b** are shown in Table 3, together with reaction yields and diastereoisomeric **a/b** ratios. The relative configuration of the cycloadducts **25a,b–35a,b** was assigned on the basis of chemical correlations and NMR analysis and was supported by semiempirical calculations (see below). Diastereoisomeric ratios were determined on the crude mixtures by ^{1}H NMR analysis and confirmed, when possible, after purification of the diastereoisomers by flash chromatography.[9] Selected ^{1}H and ^{13}C NMR data for **25a,b–35a,b** are collected in Table 4.

From the data reported in Table 3, it clearly appears that the extent of stereoselectivity is almost independent of the nature of the allylic heteroatom and sensitive mostly to steric effects. The *O*-TBDMS derivatives **5–8**, and the *O*-Ac derivatives **9–12**, show an increased *syn* selectivity in the cycloaddition reaction on passing from Me ≈ Ph < *n*-Pr < *i*-Pr (entries 1–6 and 7–10).[10,11] Another interesting observation comes from the comparison of entries 1 *vs* 7, 2 *vs* 8, 4 *vs* 9, and 6 *vs* 10: the *syn* selectivity is almost independent of the nature of the protecting group at the allylic oxygen. This behavior is significantly different from the one observed in the benzonitrile oxide cycloadditions (Table 1). For instance, in the *n*-propyl series, the nitrile oxide reaction is more *syn* selective for the TBDMS ether **6** than for the acetyl derivative **10** (Table 1, entries 6 *vs* 10); this is not true for diazomethane reactions, since almost no difference in stereoselectivity is observed (Table 3, entries 2 *vs* 8). When the R group at the allylic stereocenter is particularly small, *e.g.* in the case of methyl and phenyl derivatives, these differences are enhanced. Thus, alkene **11** reacts with both benzonitrile oxide and diazomethane with low *syn* selectivity (Table 1, entry 9, *vs* Table 3, entry 7), but alkene **5** is by far more *syn* selective when reacting with benzonitrile oxide (Table 1, entry 5, *vs* Table 3, entry 1). These data as a whole seem to suggest that electrostatic effects are attenuated in diazomethane cycloadditions with respect to benzonitrile oxide ones, while steric factors play the major role in determining the stereoselectivity of these reactions.

Some additional comments can be derived from examination of the data relative to the diazomethane cycloaddition of the alcohols **1–3** (Table 3, entries 11–14). First of all, the reaction of the other alkenes (*e.g.* alkene **6**, entries 2 *vs* 3; alkene **7**, entries 4 *vs* 5) is almost insensitive to temperature: an increased reaction temperature generally leads only to an increased chemical yield without affecting the diastereoisomeric ratio. In the case of the reaction of the alcohols **1–3**, on the other hand, the cycloadducts are quite unstable and decompose easily, thus significantly lowering the reaction yields

(11) The synthesis of the Baylis–Hillman adduct bearing a *tert*-butyl residue was also attempted by reacting methyl acrylate with pivalic aldehyde, to maximize the steric hindrance of the alkyl substituent at the allylic stereocenter. However, only traces of the desired alkene were obtained, together with rearranged products. Nevertheless, the crude was silylated and the product reacted with diazomethane, but we observed no cycloadduct formation, suggesting that the *tert*-butyl derivative is too hindered for the reaction to occur.

Table 4. Relevant ^{1}H and ^{13}C NMR Data for Products 25–35 and 37–40[a]

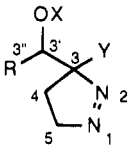

25-35, 38, 39

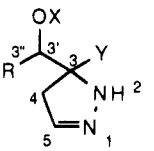

37, 40

	^{1}H			^{13}C			
	3′	4[b]	5[b]	3	3′	4	5
25a	4.75	1.72; 1.95	4.48; 4.53	105.2	70.4	19.2	78.4
25b	4.60	1.80	4.47; 4.54	102.0	70.7	17.2	77.8
26a	4.60	1.73; 2.00	4.47; 4.63	105.0	71.9	34.2	78.6
26b	4.41	1.87; 1.87	4.55; 4.65	102.3	73.2	33.5	78.0
27a	4.64	1.80; 2.15	4.46; 4.71	105.2	75.7	31.2	79.3
28a	4.96	1.78; 2.13	4.54	104.6	69.8	22.6	79.0
28b	4.83	1.81; 1.97	4.52	101.2	70.4	21.4	78.0
29a	4.94	1.78; 2.11	4.47; 4.62	106.5	72.4	37.0	79.0
29b	4.75	1.80; 2.02	4.47; 4.60	104.7	74.2	35.6	77.8
30a	4.98	1.85; 2.20	4.40; 4.72	106.3	76.3	32.2	79.5
30b	4.66	1.83; 1.93	4.43; 4.65	104.4	77.3	31.2	77.9
31a	5.86	1.86; 2.03	4.50	107.0	75.2	18.5	78.7
31b	5.77	1.86; 2.03	3.46; 4.00	106.0	75.4	18.0	77.7
32a	5.96	1.73; 2.13	4.54	103.1	70.0	22.8	78.7
32b	5.76	1.70; 1.97	4.52	100.4	71.5	20.8	78.1
33a	6.11	1.72; 2.15	4.61; 4.61	103.6	72.5	33.0	78.8
33b	5.74	1.67; 1.87	4.48; 4.48	100.5	74.2	32.4	77.7
34a	6.13	1.70; 2.26	4.50; 4.72	103.8	76.2	30.7	79.4
34b	5.53	1.66; 1.80	4.43; 4.50	99.8	76.2	30.4	79.2
35a	6.96	1.79; 2.07	3.81; 4.41	102.7	75.0	21.4	78.2
35b	6.80	1.83; 1.98	4.30; 4.46	102.2	75.5	20.8	78.2
37a	3.94	2.82; 3.11	6.64	77.0	143.0	37.6	74.2
37b	3.86	2.62; 3.09	6.66	75.5	142.9	40.0	74.2
38a	4.23	1.40; 1.63	4.46	102.2	71.4	33.9	78.1
38b	4.01	1.46; 1.66	4.46	100.0	73.7	33.7	77.8
39a	4.45	1.27; 1.71	4.45	102.0	72.2	36.4	78.5
39b	4.17	1.46; 1.60	4.44	101.8	73.1	35.7	77.4
40a	3.68	2.68	6.70	70.0	145.0	39.6	76.0

[a] Chemical shifts in ppm from TMS. **37** and **40** are given the same numbering system of **25–35** to compare more easily their ^{1}H and ^{13}C chemical shifts with those of compounds **25–35**, **38** and **40**. [b] AB system.

(entries 12 *vs* 13). The decomposition reaction seems to proceed via an elimination of the aldehyde residue; an interesting consequence of this instability was the synthesis of the bicyclic product **36a,b** (see below). Even at 0 °C, the cycloaddition of alkenes **1–3** with diazomethane often shows poor chemical yields, despite the attention used in performing the reaction and in isolating the products. In the particular case of cycloadducts **26a,b**, the **a/b** ratio is the same at 0 and 25 °C, but these products are significantly more stable than the corresponding **25a,b** and **27a,b**. The cycloadduct between diazomethane and alkene **4** was observed via TLC but was never isolated and characterized because of its instability (entry 15). We cannot exclude that in these cases the decomposition rate is different for the two **a** and **b** diastereoisomers, since the chemical yield is always very low; thus, no significant conclusions about the stereoselectivity of these reactions can be drawn. In the case of alkene **2**, however, chemical yields were good when the reaction was carried out at 0 °C; in this case, the trend observed for the *n*-propyl derivatives (entries 2 *vs* 8 *vs* 12) suggests a small influence of the size of the residue at the oxygen: the smaller the size of the X group, the higher the *syn* stereoselectivity.

NMR Analysis and Relative Configuration Assignment to 25a,b–35a,b. The ^{1}H and ^{13}C NMR data of compounds **25a,b–35a,b** are reported in Table 4. The structural assignments were based on ^{13}C chemical shifts and DEPT[12] experiments, by comparison with NMR data of related compounds.[13] The coupling constants were similar in all compounds; thus, they were not diagnostic for the assignment of the relative configuration. Instead, the ^{1}H and ^{13}C spectra exhibited significantly different signals for **a** and **b** diastereoisomers. H3′, C3, C3′, and C4 of **a** isomers were shifted downfield up to $\Delta\delta = 0.37$ (for ^{1}H) and 3.1 (for ^{13}C) with respect to the **b** isomers. The NMR trends observed for each **a,b** pair supported the assignment of the same relative configuration to the major **a** isomers in all of the cycloadducts.

Chemical correlation between **26a**, **29a**, and **33a** confirmed this hypothesis (Scheme 3). Silylation of an 80/20 mixture of cycloadducts **26a,b** with TBDMSCl in the presence of imidazole gave an 80/20 mixture of **29a,b**. On the other hand, when desilylation of **29a,b** to obtain **26a,b** was attempted, only the isomerized 2-pyrazolines **37a,b** were isolated. Reaction of **37a,b** with HF gave some desilylated product but in unreasonably low yields. Any attempt to acylate **26a** to give **33a** was unsuccessful: **26a** underwent isomerization of the pyrazolinic ring and a retro-addition reaction that eliminated butyraldehyde. This reacted with the aminoalcohol, affording the unexpected cyclic emiaminal **36a**, which was fully characterized (see below). In a similar way **36b** was obtained from **26b**. Selected ^{1}H and ^{13}C NMR data for **36a,b** are collected in Table 5; selected data for **37a,b** are included in Table 4. To chemically correlate **26a** and **33a**, both were reduced to diol **38a** by treatment with DIBAL-H. Thus, all **a** isomers in the *n*-propyl series have the same relative configuration at the stereocenters. On the basis of the observed NMR trends (Table 4), this conclusion can be extended to all **a** isomers.

Scheme 3. Chemical Correlations of Diazomethane Cycloaddition Products (Only Major *syn* Isomers Are Shown for Simplicity)

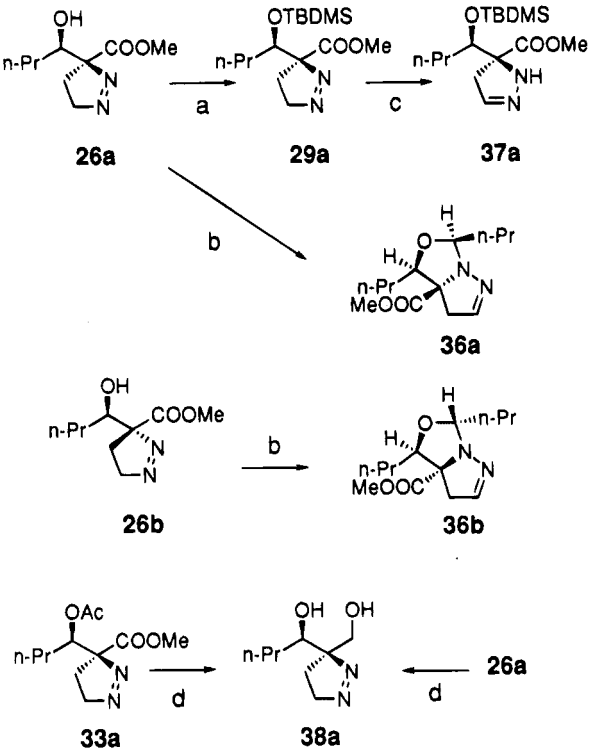

a) TBDMSCl, imidazole, DMF; b) AcCl, Py, CH_2Cl_2; c) HF, CH_3CN; d) DIBALH, CH_2Cl_2.

The definitive assignment of the relative *syn* and *anti* configuration to isomers **a** and **b**, respectively, was not an easy task. First of all, it must be noted that the inside alkoxy theory predicts the preferential formation of the *syn* cycloadducts and that the transition state conformation featuring the oxygen in the *inside* position and the alkyl residue *anti* should be favored also for steric reasons. The inside alkoxy, *syn* products are indeed the major ones in the corresponding nitrile oxide cycloadditions (Table 1). Moreover, it is well-known[1] that the stereoselectivity of these cycloadditions mainly depends on the nature of the alkene—in other words, the 1,3-dipole influences only the extent, and not the sense, of the stereoselectivity. Therefore, it is reasonable to presume that also in the case of diazomethane cycloadditions the **a** products have a 3,3′-*syn* relative configuration. Nevertheless, experimental support of this assignment was needed.

In a first attempt **38a** (synthesized by reduction of **26a** or **33a** with DIBAL-H) was treated with 2,2-dimethoxypropane in the presence of PTSA (Scheme 4) with the goal of obtaining a product (**1st synthetic target**) that presents the two stereocenters locked in a rigid bicyclic ring, so that the NOE analysis should reveal its relative configuration. This is analogous to the procedure followed by Kanemasa *et al.*[8] for determining the 5–5′ relative configuration of compounds **13a,b**. However, despite the mild acidic conditions, **38a** gave a complex mixture of products, which were not identified. In a parallel experiment to obtain **38a**, the carboxylic ester of **29a** was reduced to the corresponding alcohol **39a** by treatment with DIBAL-H. Upon treatment with HF 30% in THF or acetonitrile, however, only 2-pyrazoline **40a** was obtained, the TBDMS residue now protecting the

(12) Doddrel, D. M.; Pegg, D. T.; Bendall, M. R. *J. Magn. Reson.* **1982**, *48*, 323.
(13) Kalinowski, H. O.; Berger, S.; Braun, S. *Carbon–13 NMR Spectroscopy*; Wiley: New York, 1988.
(14) Edwards, M. W.; Bax, A. *J. Am. Chem. Soc.* **1986**, *108*, 918.
(15) Bax, A.; Subramanian, S. *J. Magn. Reson.* **1986**, *67*, 565.
(16) Bax, A.; Summers, M. F. *J. Am. Chem. Soc.* **1986**, *108*, 2094.

Table 5. Relevant ^1H and ^{13}C NMR Data for Products 36 and 41[a]

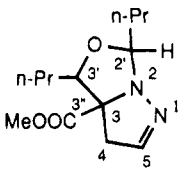

36a,b

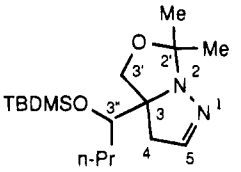

41a,b

	^1H				^{13}C					
	3″	4[b]	5	3′	3	3″	4	5	3′	2′
36a		2.96; 3.20	6.80	3.93	76.4	173.3	39.0	145.2	80.7	95.2
36b		3.00; 3.28	6.83	3.70	76.2	173.0	43.4	145.0	82.3	95.4
41a	3.77	3.49; 3.20	6.80	3.59; 3.74	76.7	72.3	41.7	145.0	72.3	97.8
41b	3.80	2.56; 2.70	6.75	3.53; 3.93	76.6	74.1	41.6	145.4	74.1	97.6

[a] Chemical shifts in ppm from TMS. The procedure for the assignment of NMR spectra involved (i) assignment of the ^1H NMR using homonuclear Hartmann–Hann (HOHAHA) experiment (ref 14), (ii) correlation *via* $^1J(C-H)$ using ^1H-detected heteronuclear multiple-quantum coherence (HMQC; ref 15) to provide the ^{13}C assignment of the protonated C atoms, and (iii) correlation *via* $^2J(C-H)$ and $^3J(C-H)$ using heteronuclear multiple-bond correlation (HMBC; ref 16) to assign nonprotonated C atoms and verify the consistency of the ^1H and ^{13}C assignment made using the above-mentioned techniques. [b] AB system.

Scheme 4. Attempted Synthesis of Rigid Bicyclic Adducts from 1-Pyrazolines for NOE Experiments

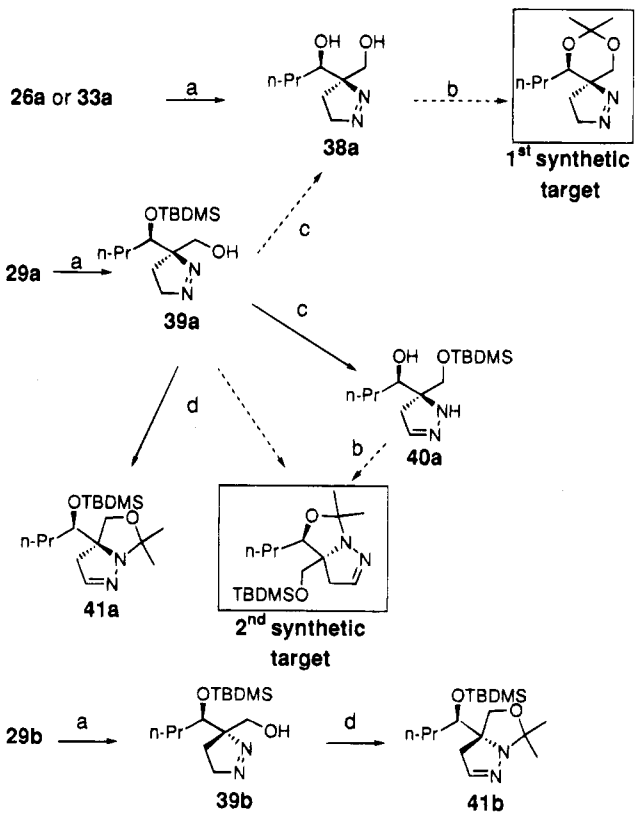

a) DIBALH, CH_2Cl_2; b) $(MeO)_2CMe_2$, PTSA; c) HF, CH_3CN or THF; d) $(MeO)_2CMe_2$, HF.

primary alcohol and the pyrazolinic ring being isomerized by the acidic conditions. Any other attempt to desilylate **39a** by using a different procedure (*e.g.* Bu_4NF in THF) led only to complete decomposition of the product.

We envisioned at this point the synthesis of another substrate (**2nd synthetic target**) equally suitable for NOE assignment of the relative stereochemistry; however, treatment of **40a** with 2,2-dimethoxypropane and PTSA resulted in the formation of decomposition products. In the one-pot treatment of **39a** with 2,2-dimethoxypropane and HF, on the other hand, no shift of the TBDMS protecting group from the secondary to the primary alcohol was observed: only the emiaminal **41a** was isolated. Starting from **29b**, the corresponding diastereoisomer **41b** was formed, and of course the two exhibited similar NOE patterns for the *n*-PrCH(OTBDMS) residue. Selected ^1H and ^{13}C NMR data for **39a,b**, **40a,b**, and **41a,b** are collected in Tables 4 and 5. A serendipitous solution to this problem came in the meanwhile from NMR analysis of **36a** and **36b**, unexpectedly obtained by treatment of **26a** and **26b**, respectively, in an attempt to acetylate the hydroxy group with acetyl chloride in the presence of pyridine (Scheme 3).

The use of the NOE effect for determining interproton distances and molecular structures is well established.[17] In our case, the NOE measurements involving H3′ and related protons were suitable for a clear assignment of the 3–3′ relative configuration to isomers **36a** and **36b**. The 2D NOE phase sensitive pulse sequence[18] was used; the mixing time, τ_m, allowed for magnetization exchange due to dipole–dipole relaxation between two spins. Several 2D NOESY experiments were performed with τ_m in the order of spin–lattice relaxation time to evaluate the dipolar interaction (NOE effect) as the intensity of the off-diagonal peaks and with $\tau_m = 0$ to value the equilibrium magnetization as the intensity of the diagonal peaks.[19] The 2D NOESY spectra recorded with τ_m = 1.4 s showed interaction between H3′,H2′ and H4a,CH_2-Et on the stereocenter 3′ for the major isomer **36a**, while the H3′ proton revealed NOE with H4a in the minor isomer **36b** (Figure 3). Moreover, we applied the equation $r_{ij}^6/r_{kl}^6 = NOE_{kl}/NOE_{ij}$[17] which well relates the NOEs and the interproton distances under condition of prevalent dipole–dipole interactions and isotropic overall molecular motion. Using the geminal protons H4a and H4b, separated by a known distance[20] of 1.77 Å, as internal reference, the interproton distances between H3′,H2′ and H4a,3′-CH_2Et were found to be 2.21 and 1.72

(17) Noggle, J. H.; Schirmer, R. E. *The Nuclear Overhauser Effect*; Academic Press: New York, 1971.
(18) States, D. J.; Haberkorn, R. A.; Ruben, D. J. *J. Magn. Reson.* **1982**, *48*, 286.
(19) (a) Kumar, A.; Wagner, G.; Ernst, R. R.; Wuthrich, K. *J. Am. Chem. Soc.* **1981**, *103*, 3654. (b) Keepers, J. W.; James, T. L. *J. Magn. Reson.* **1984**, *54*, 404.
(20) (a) Wagner, G.; Wuthrich, K. *J. Magn. Reson.* **1979**, *33*, 675. (b) Braun, W.; Bosch, C.; Brown, L. R.; Go, N.; Wuthrich, K. *Biochim. Biophys. Acta* **1981**, *667*, 377.

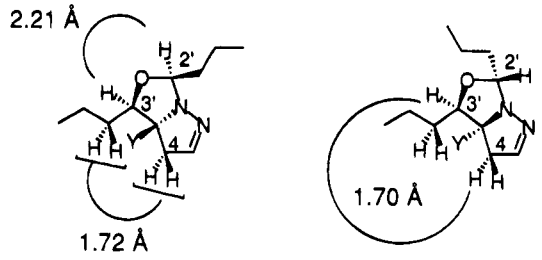

36a **36b**

Figure 3. Relevant NOE-derived H–H distances for compounds **36a,b** (Y = COOMe).

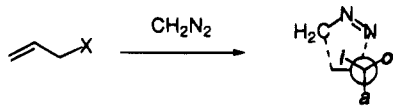

	X = Me	X = OMe
inside	1.2	0.0
anti	0.0	0.3
outside	0.4	(0.8)

Figure 4. PM3 relative energies of the transition structures for diazomethane cycloadditions to alkenes (kcal/mol).

Å, respectively, for **36a**, and 1.70 Å for H3′,H4a for **36b** isomer; all distances are evaluated with a ±0.3 Å uncertainty. The proximity of H3′,H2′ protons and of H4a with the 3′-*n*-propyl moiety in **36a** was evidence for its relative configuration shown in Scheme 3; the absence of this interaction in **36b** and of any interaction of H3′ with the carbomethoxy substituent supported this assignment. In **36b** a proximity of H3′ and H4a was revealed in agreement with the structure shown in Figure 3. Thus, the *syn* relative configuration at the 3–3′ stereocenters of the major diastereoisomers **25a-35a** was fully established, as was the *anti* relative configuration of the minor isomers **25b–35b**.

Evaluation of the Diastereoisomeric Ratio via PM3 Calculations. We also performed semiempirical calculations to correlate the experimentally observed diastereoselectivity in the diazomethane cycloadditions to the calculated diastereoisomeric ratios. We were particularly interested in testing the performance of semiempirical procedures in this kind of reaction: semiempirical methods are by far more practical to use than *ab initio* method, and allow the treatment of molecular structures of relevant size. On the other hand, it is well-known that the use of semiempirical Hamiltonians is not always reliable when dealing with cycloaddition reactions. From the recent literature[21] we found PM3[22] to be quite promising in this respect. Thus, we proceeded to locate transition structures for the reaction of diazomethane with chiral allyl ethers using the Hamiltonian PM3 as implemented in MOPAC 6.0.[23] The search for the transition structures started from the diazomethane plus ethylene structure[6,21] (Figure 2) by addition of the residues in the proper position and conformation. All variables were optimized, and the stationary points were characterized as transition structures by performing a vibrational analysis, which showed the existence of only one negative frequency corresponding to the symmetric stretch of the two forming bonds.

First of all, we located the six transition structures for the reaction of 1-butene with diazomethane to evaluate the conformational preferences for a methyl group in the transition structure. As in the nitrile oxide cycloadditions, the methyl residue—a model for an alkyl substituent—prefers to occupy the *anti* position, the *inside* being the most disfavored one (1.2 kcal/mol higher in energy). The relative energies are reported in Figure 4. This behavior is the same reported for nitrile oxide cycloadditions (Figure 1).[2] When the same calculation was performed with allylic alcohol as a model for methyl allyl ether (by fixing the C–C–O–H dihedral angle to 180°), the oxygenated residue was found to preferentially occupy the *inside* position rather than the *anti* position, destabilized by only 0.3 kcal/mol. No staggered conformations corresponding to an *outside* location of the oxygen were found on this potential energy surface.[3,24] By fixing the dihedral angles at the allylic residue in a staggered conformation, the relative energy of the *outside* conformation rises to 1.3 kcal/mol, a value lower than the corresponding one for the *outside* conformation of the nitrile oxide transition structure (Figure 1).[2,4]

We then proceeded to locate the PM3 transition structures for the cycloaddition of diazomethane with 3-methoxy-1-butene, as usual modeled with 3-buten-2-ol by constraining the C–C–O–H dihedral angle to 180°. The six transition structures, leading to the *syn* (**A–C**) and *anti* (**A′–C′**) isomers, are shown in Figure 5 with their relative energy values in kilocalories per mole. The calculated diastereoisomeric ratio at 273 K was 76/24 in favor of the inside alkoxy product, in fairly good agreement with the experimental results for the methyl derivatives (Table 3, entries 1 and 7).[25] It is interesting to note that PM3 calculations seem to be qualitatively

(21) Sustmann, R.; Sicking, W.; Felderhoff, M. *Tetrahedron* **1990**, *46*, 783.

(22) Stewart, J. J. P. *J. Comput. Chem.* **1989**, *10*, 221. For additional references to semiempirical Hamiltonians, see: *Reviews in Computational Chemistry;* Lipkowitz, K. B., Boyd, D. B., Eds.; VCH Publishers: Weinheim, Germany, 1990 (Vol. 1 Chapter 2), 1991 (Vol. 2 Chapter 8).

(23) Stewart, J. J. P. MOPAC 6.0. QCPE Program 455.

(24) We located a conformation, 0.8 kcal/mol higher in energy than the *inside* one, bearing the oxygen in the *outside* region; in this conformation, however, staggering of the forming bonds with respect to the allylic stereocenter is lost. This new conformation is more similar to the *anti* than to the *outside* one. The PM3 data for the diazomethane cycloaddition are not directly comparable to the *ab initio* data reported in Figure 1 for the nitrile oxide cycloaddition; thus, we optimized the three conformations (*inside*, *outside*, and *anti*) for the fulminic acid plus allylic alcohol transition structure (*cf.* Figure 1) at the PM3 level. Also in this case, all variables but the C–C–O–H dihedral, fixed at 180°, were optimized. The *inside* conformation is 0.4 kcal/mol higher in energy than the *anti* one, and no *outside* conformation was located on the potential energy surface.

(25) We performed PM3 calculations also on the aldehyde MeCH(OH)C(=CH_2)CHO, which is probably a better model for the reactions of **1–12** with diazomethane. However, with this CHO residue achievement of convergence in PM3 calculation was significantly more difficult than with the unactivated alkene. Besides, the *s-cis* and *s-trans* conformations for the α,β-unsaturated system must be considered in the TS. In the ground state, *s-cis*-metacrolein was found to be more stable than the *s-trans* by 0.5 kcal/mol at the PM3 level. From the energy data obtained in a partial optimization of the six transition structures deriving from the *s-cis* conformation of the aldehyde only (the two forming bonds were fixed to the corresponding value for the diazomethane plus ethylene transition structure),[6] the favored product was the inside alkoxy, *syn* one, the calculated *syn*/*anti* diastereoisomeric ratio being 89/11 (a value slightly higher than the experimental one; cf. Table 3). We also located the TS for the reaction of MeCH(OH)C(=CH_2)Me with diazomethane: after a full optimization of all variables, we evaluated the diastereoselectivity as 90/10 favoring the *syn* adduct.

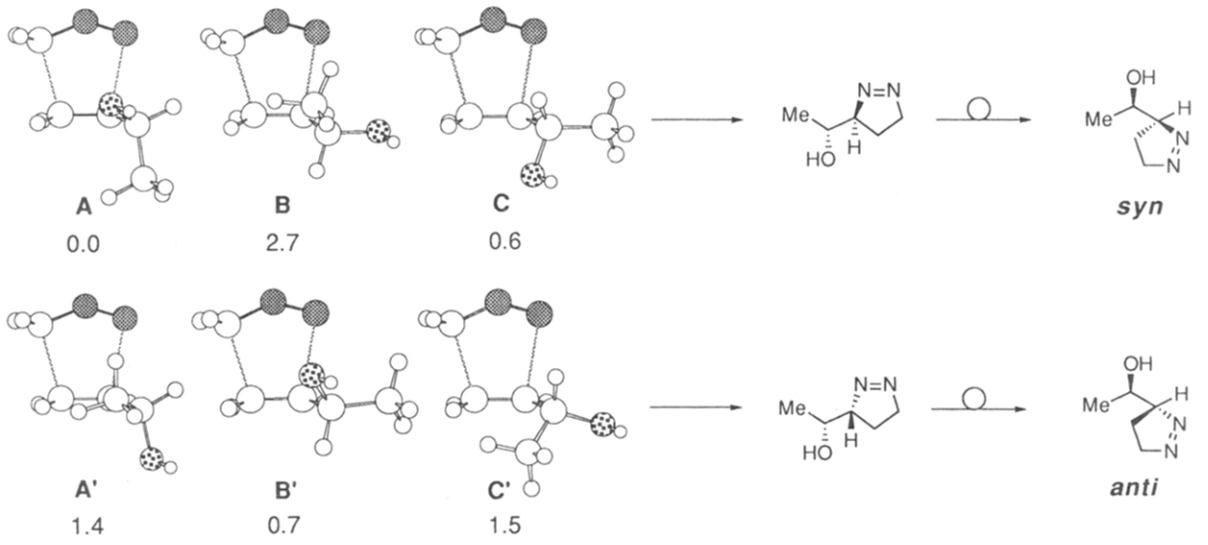

Figure 5. Relative energies (kcal/mol) for the six diazomethane *plus* 3-hydroxy-1-butene PM3 transition structures.

reliable and to offer an easy tool to evaluate the conformational preferences in the transition states of these reactions.

Conclusions

From the experimental and calculated data here reported, some conclusions can be drawn for the 1,3-dipolar cycloaddition of diazomethane to chiral allyl ethers: (i) The general assumptions of the inside alkoxy theory[1-4] allow a correct prediction of the sense of the diastereoselectivity, since the major *syn* isomers are the ones predicted by the inside alkoxy theory. (ii) The extent of selectivity seems to depend more on steric than on stereoelectronic factors, which play a reduced role with respect to the corresponding nitrile oxide cycloadditions.[1-4,8] This may be due to the reduced negative charge on the terminal nitrogen of the 1,3-dipole.[6] (iii) In the diazomethane cycloadditions to allyl TBDMS ethers and to allyl esters, the same amount of stereoselectivity was achieved, while for nitrile oxide cycloadditions the TBDMS ethers are more *syn* selective. This can be ascribed to the reduced electrostatic repulsion between the charged terminus of the 1,3-dipole and the heteroatom in the allylic position.

Experimental Section

^{1}H NMR spectra of compounds **1**−**12** were recorded at 80 MHz, ^{1}H spectra of compounds **13**−**41** were recorded at 300 MHz, and ^{13}C NMR spectra were recorded at 75.43 MHz. All spectra were recorded in $CDCl_3$ as solvent, and chemical shifts are reported in δ relative to TMS.

Silica gel (230−400 mesh ASTM) was used for flash chromatography. Organic extracts were dried over Na_2SO_4 and filtered before removal of the solvent. All reactions employing dry solvents were run under nitrogen: THF was distilled twice from Na, Et_2O from Na and subsequently from $LiAlH_4$, and CH_2Cl_2 from CaH_2; these solvents were stored on molecular sieves. Commercial dry DMF and acetonitrile were used without additional purification and stored on molecular sieves; pyridine was stored on KOH.

Diazomethane was prepared in small quantities as ethereal solution (0.4 M), with particular caution due to the risks of explosions, and was never stored: any amount of unused solution was immediately destroyed with acetic acid. All reactions with diazomethane were performed in the dark and under a safety hood.

1−**4** were known compounds and were synthesized by reacting methyl crotonate with the proper aldehyde for 7−10 days in the presence of catalytic DABCO; the crude allylic alcohols **1**−**4** were obtained in about 50% yield and purified (when needed) by flash chromatography. Their spectroscopic characterization was in agreement with published data.[7,26]

General Procedure for the Synthesis of 5−**8 (Scheme 1).** To alcohols **1**−**4** (1 mmol) in dry DMF (0.3 mL) were added 2 mmol of TBDMSCl and 2.5 mmol of imidazole, and the mixture was allowed to stir at room temperature for 24 h. Water was added, and the product was extracted with Et_2O.

(a) Methyl 3-[(*tert*-butyldimethylsilyl)oxy]-2-methylenebutanoate (5) was obtained in 75% yield after flash chromatography (hexanes/Et_2O = 9/1): IR 2950, 2800, 1730, 1600 cm^{-1}; ^{1}H NMR δ 6.15 (bt, 1H), 5.90 (bt, 1H), 4.65 (bq, 1H), 3.70 (s, 3H), 1.25 (d, 3H, J = 7.0 Hz), 0.85 (s, 9H), 0.50 (s, 3H), 0.00 (s, 3H). Anal. Calcd for $C_{12}H_{24}O_3Si$: C, 58.97; H, 9.90. Found: C, 58.88; H, 9.94.

(b) Methyl 3-[(*tert*-butyldimethylsilyl)oxy]-2-methylenesanoate (6) was obtained in 89% yield as an oil and used without further purification: IR 2950, 2850, 1730, 1610 cm^{-1}; ^{1}H NMR δ 6.20 (bd, 1H), 5.85 (bt, 1H), 4.60 (bt, 1H), 3.75 (s, 3H), 1.40 (m, 4H), 0.85 (m, 12H), 0.05 (s, 3H), 0.00 (s, 3H). Anal. Calcd for $C_{14}H_{28}O_3Si$: C, 61.72; H, 10.36. Found: C, 61.75; H, 10.38.

(c) Methyl 3-[(*tert*-butyldimethylsilyl)oxy]-4-methyl-2-methylenepentanoate (7) was obtained as an oil in 45% yield after purification by flash chromatography (hexanes/Et_2O = 9/1): IR 2950, 2850, 1730, 1610, 1350 cm^{-1}; ^{1}H NMR δ 6.30 (bd, 1H), 5.80 (bt, 1H), 4.40 (bd, 1H), 3.72 (s, 3H), 1.60 (m, 1H), 0.90 (d, 3H, J = 7.0 Hz), 0.90 (s, 9H), 0.03 (s, 3H), 0.00 (s, 3H). Anal. Calcd for $C_{14}H_{28}O_3Si$: C, 61.72; H, 10.36. Found: C, 61.70; H, 10.37.

(d) Methyl 3-[(*tert*-butyldimethylsilyl)oxy]-3-phenyl-2-methylenepropanoate (8) was obtained in 60% yield after flash chromatography (hexanes/Et_2O = 9/1): IR 3100, 2900, 2800, 1720, 1610 cm^{-1}; ^{1}H NMR δ 7.30 (m, 5H), 6.25 (bt, 1H), 6.15 (bt, 1H), 5.60 (bt, 1H), 3.65 (s, 3H), 0.90 (s, 9H), 0.00 (s, 3H), −0.10 (s, 3H). Anal. Calcd for $C_{17}H_{26}O_3Si$: C, 66.62; H, 8.55. Found: C, 66.58; H, 8.59.

General Procedure for the Synthesis of 9−**12 (Scheme 1).** To a solution of alcohols **1-4** (1 mmol) in dry CH_2Cl_2 were added 1.1 mmol of pyridine and 1.1 mmol of AcCl at 0 °C. After 1 h, the mixture was treated with 3.7% HCl and extracted with CH_2Cl_2. The crude products were purified by flash chromatography when needed.

(a) Methyl 3-acetoxy-2-methylenebutanoate (9) was obtained in 67% yield after flash chromatography (hexanes/

(26) (a) Calderón, A.; Font, J.; de March, P. *Tetrahedron* **1992**, *48*, 5347. (b) Wang, S.-Z.; Yamamoto, K.; Yamada, H.; Takahashi, T. *Tetrahedron* **1992**, *48*, 2333.

Et_2O = 8/2): IR 2950, 2850, 1750, 1600 cm^{-1}; ^1H NMR δ 6.20 (s, 1H), 5.80 (s, 1H), 5.60 (q, 1H, J = 7.0 Hz), 3.75 (s, 3H), 2.07 (s, 3H), 1.35 (d, 3H, J = 7.0 Hz). Anal. Calcd for $C_8H_{12}O_4$: C, 55.80; H, 7.02. Found: C, 55.86; H, 6.98.

(b) Methyl 3-acetoxy-2-methylenesanoate (10) was obtained in 86% yield as an oil and used without further purification: IR 3000, 2900, 1750, 1610 cm^{-1}; ^1H NMR δ 6.20 (s, 1H), 5.80 (s, 1H), 3.70 (s, 3H), 2.05 (s, 3H), 1.50 (m, 4H), 0.90 (bt, 3H). Anal. Calcd for $C_{10}H_{16}O_4$: C, 59.98; H, 8.05. Found: C, 60.01; H, 8.04.

(c) Methyl 3-acetoxy-4-methyl-2-methylenepentanoate (11) was obtained as an oil in 60% yield after flash chromatography (hexanes/Et_2O = 8/2): IR 3000, 2850, 1750, 1610, 1400 cm^{-1}; ^1H NMR δ 6.25 (s, 1H), 5.57 (s, 1H), 5.40 (d, 1H, J = 5.9 Hz), 3.70 (s, 3H), 2.05 (s, 3H), 2.00 (m, 1H), 0.95 (d, 3H, J = 5.9 Hz), 0.90 (d, 3H, J = 5.9 Hz). Anal. Calcd for $C_{10}H_{16}O_4$: C, 59.98; H, 8.05. Found: C, 59.95; H, 8.07.

(d) Methyl 3-acetoxy-3-phenyl-2-methylenepropanoate (12) was obtained quantitatively and used without further purification: IR 3100, 3050, 2950, 2850, 1750, 1720, 1610 cm^{-1}; ^1H NMR δ 7.30 (s, 5H), 6.65 (s, 1H), 6.40 (s, 1H), 5.85 (s, 1H), 3.70 (s, 3H), 2.10 (s, 3H). Anal. Calcd for $C_{13}H_{14}O_4$: C, 66.66; H, 6.02. Found: C, 66.71; H, 5.99.

General Procedure for the Cycloaddition Reaction of Benzonitrile Oxide to Alkenes 1–12 To Give 4,5-Dihydroisoxazoles 13a,b–24a,b (Table 1). To a stirred solution of the desired alkene (1 mmol) and phenyl hydroxamoil chloride (3.5 mmol, 544 mg) in Et_2O (10 mL) cooled at 0 °C was added triethylamine (7.4 mmol, 1 mL) dropwise. The reaction mixture was left at 0 °C for 3–6 h and then filtered. The crudes were purified by flash chromatography. Chemical yields and diastereoisomeric ratios are collected in Table 1; significant ^1H and ^{13}C NMR data are collected in Table 2.

(a) 5-Carbomethoxy-5-(1′-hydroxyethyl)-4,5-dihydroisoxazoles (13a,b): hexanes/Et_2O = 1/1; IR 3400, 3000, 2850, 1740 cm^{-1}. Anal. Calcd for $C_{13}H_{15}NO_4$: C, 62.64; H, 6.07; N, 5.62. Found: C, 62.68; H, 6.09; N, 5.60.

(b) 5-Carbomethoxy-5-(1′-hydroxybutyl)-4, 5-dihydroisoxazoles (14a,b): hexanes/Et_2O = 6/4; IR 3400, 2950, 2850, 1730 cm^{-1}. Anal. Calcd for $C_{15}H_{19}NO_4$: C, 64.96; H, 6.91; N, 5.05. Found: C, 64.92; H, 6.92; N, 5.08.

(c) 5-Carbomethoxy-5-(1′-hydroxy-2′-methylpropyl)-4,5-dihydroisoxazoles (15a,b): hexanes/Et_2O = 6/4; IR 3350, 2900, 2800, 1740, 1590 cm^{-1}. Anal. Calcd for $C_{15}H_{19}NO_4$: C, 64.96; H, 6.91; N, 5.05. Found: C, 65.00; H, 6.89; N, 5.09.

(d) 5-Carbomethoxy-5-(1′-hydroxy-1′-phenylmethyl)-4,5-dihydroisoxazoles (16a,b): hexanes/Et_2O = 6/4; IR 3400, 3050, 2950, 2850, 1740 cm^{-1}. Anal. Calcd for $C_{18}H_{17}NO_4$: C, 69.44; H, 5.50; N, 4.50. Found: C, 69.47; H, 5.53; N, 4.45.

(e) 5-Carbomethoxy-5-[1′-[(*tert*-butyldimethylsilyl)oxy]ethyl]-4,5-dihydroisoxazoles (17a,b): hexanes/Et_2O = 8/2; IR 3000, 2900, 2800, 1750 cm^{-1}. Anal. Calcd for $C_{19}H_{29}NO_4Si$: C, 62.78; H, 8.08; N, 3.85. Found: C, 62.84; H, 8.10; N, 3.81.

(f) 5-Carbomethoxy-5-[1′-[(*tert*-butyldimethylsilyloxy]butyl]-4,5-dihydroisoxazoles (18a,b): hexanes/Et_2O = 9/1; IR 3050, 2950, 2800, 1730, 1600 cm^{-1}. Anal. Calcd for $C_{21}H_{33}NO_4Si$: C, 64.41; H, 8.50; N, 3.58. Found: C, 64.37; H, 8.55; N, 3.60.

(g) 5-Carbomethoxy-5-[1′-[(*tert*-butyldimethylsilyl)oxy]-2′-methylpropyl]-4,5-dihydroisoxazoles (19a,b): hexanes/Et_2O = 8/2; IR 3080, 2960, 2860, 1740, 1600 cm^{-1}. Anal. Calcd for $C_{21}H_{33}NO_4Si$: C, 64.41; H, 8.50; N, 3.58. Found: C, 64.46; H, 8.44; N, 3.61.

(h) 5-Carbomethoxy-5-[1′-[(*tert*-butyldimethylsilyl)oxy]-1′-phenylmethyl]-4,5-dihydroisoxazoles (20a,b): hexanes/Et_2O = 8/2; IR 3050, 2920, 2800, 2300, 1740, 1600 cm^{-1}. Anal. Calcd for $C_{24}H_{31}NO_4Si$: C, 67.73; H, 7.34; N, 3.29. Found: C, 67.75; H, 7.36; N, 3.26.

(i) 5-Carbomethoxy-5-(1′-acetoxyethyl)-4, 5-dihydroisoxazoles (21a,b): hexanes/Et_2O = 6/4; IR 3100, 2900, 1750 cm^{-1}. Anal. Calcd for $C_{15}H_{17}NO_5$: C, 61.85; H, 5.88; N, 4.81. Found: C, 61.90; H, 5.90; N, 4.79.

(j) 5-Carbomethoxy-5-(1′-acetoxybutyl)-4,5-dihydroisoxazoles (22a,b): hexanes/Et_2O = 7/3; IR 3000, 2800, 2300, 1750 cm^{-1}. Anal. Calcd for $C_{17}H_{21}NO_5$: C, 63.94; H, 6.63; N, 4.39. Found: C, 63.90; H, 6.65; N, 4.41.

(k) 5-Carbomethoxy-5-(1′-acetoxy-2′-methylpropyl)-4,5-dihydroisoxazoles (23a,b): hexanes/Et_2O = 6/4; IR 3050, 2950, 1750 cm^{-1}. Anal. Calcd for $C_{17}H_{21}NO_5$: C, 63.94; H, 6.63; N, 4.39. Found: C, 63.99; H, 6.60; N, 4.35.

(l) 5-Carbomethoxy-5-(1′-acetoxy-1′-phenylmethyl)-4,5-dihydroisoxazoles (24a,b): hexanes/Et_2O = 6/4; IR 3100, 2900, 1750 cm^{-1}. Anal. Calcd for $C_{20}H_{19}NO_5$: C, 67.98; H, 5.42; N, 3.96. Found: C, 68.04; H, 5.40; N, 3.95.

Chemical Correlation between 13a, 17a, and 21a (Scheme 2). Compound **13a** was silylated according to the procedure described for the synthesis of **5–8**. **17a** was obtained in 30% yield after purification by flash chromatography (hexanes/Et_2O = 8/2). Compound **13a** was also treated with AcCl and pyridine in CH_2Cl_2 (see preparation of **9–12**) to give **21a** in 33% yield after flash chromatography (hexanes/Et_2O = 6/4).

General Procedure for the Cycloaddition Reaction of Diazomethane to Alkenes 1–12 To Give 1-Pyrazolines 25a,b–35a,b (Table 3). The desired alkene (1 mmol) was added to 25 mL of diazomethane solution in Et_2O (0.4 M) at 0 °C. This temperature was maintained if required (see Table 3); alternatively, the reaction was allowed to stand at room temperature. After 1–2 h, the reaction was completed. In the synthesis of compounds **28a,b–35a,b**, acetic acid was added in stoichiometric quantity to destroy the excess of diazomethane; the solvent was removed and the crude purified by flash chromatography. Compounds **25a,b–27a,b**, on the other hand, revealed a strong instability to acidic conditions: the workup of the reaction thus consisted simply in removal of Et_2O and excess CH_2N_2 under reduced pressure. All products were obtained as pale yellow oils after flash chromatography. Reaction temperatures, chemical yields, and diastereoisomeric ratios are collected in Table 3; significant ^1H and ^{13}C NMR data are collected in Table 4.

(a) 3-Carbomethoxy-3-(1′-hydroxyethyl)-1-pyrazolines (25a,b) decomposed on silica gel; thus, all analyses were performed on the crude product only: IR 3400, 2900, 2850, 2800, 1740, 1680 cm^{-1}. Anal. Calcd for $C_7H_{12}N_2O_3$: C, 48.83; H, 7.02; N, 16.27. Found: C, 48.88; H, 7.07; N, 16.21.

(b) 3-Carbomethoxy-3-(1′-hydroxybutyl)-1-pyrazolines (26a,b) were purified by flash chromatography (hexanes/Et_2O = 3/7): IR 3500, 3000, 1750, 1650 cm^{-1}. Anal. Calcd for $C_9H_{16}N_2O_3$: C, 53.98; H, 8.05; N, 13.99. Found: C, 54.00; H, 8.02; N, 14.01.

(c) 3-Carbomethoxy-3-(1′-hydroxy-2′-methylpropyl)-1-pyrazoline (27a) was purified by flash chromatography (hexanes/Et_2O = 4/6): IR 3450, 2950, 1750, 1650, 1350 cm^{-1}. Anal. Calcd for $C_9H_{16}N_2O_3$: C, 53.98; H, 8.05; N, 13.99. Found: C, 53.95; H, 8.06; N, 13.95.

(d) 3-Carbomethoxy-3-[1′-[(*tert*-butyldimethylsilyl)oxy]ethyl]-1-pyrazolines (28a,b) were purified by flash chromatography (hexanes/Et_2O = 8/2): IR 2950, 2850, 2800, 1740 cm^{-1}. Anal. Calcd for $C_{13}H_{26}N_2O_3Si$: C, 54.51; H, 9.15; N, 9.78. Found: C, 54.47; H, 9.18; N, 9.84.

(e) 3-Carbomethoxy-3-[1′-[(*tert*-butyldimethylsilyl)oxy]butyl]-1-pyrazolines (29a,b) were purified by flash chromatography (hexanes/Et_2O = 85/15): IR 2950, 1750, 1650 cm^{-1}. Anal. Calcd for $C_{15}H_{30}N_2O_3Si$: C, 57.28; H, 9.62; N, 8.91. Found: C, 57.31; H, 9.64; N, 8.95.

(f) 3-Carbomethoxy-3-[1′-[(*tert*-butyldimethylsilyl)oxy]-2′-methylpropyl]-1-pyrazolines (30a,b) were purified by flash chromatography (hexanes/Et_2O = 85/15): IR 2950, 1750, 1650, 1400 cm^{-1}. Anal. Calcd for $C_{15}H_{30}N_2O_3Si$: C, 57.28; H, 9.62; N, 8.91. Found: C, 57.30; H, 9.60; N, 8.89.

(g) 3-Carbomethoxy-3-[1′-[(*tert*-butyldimethylsilyl)oxy]-1′-phenylmethyl]-1-pyrazolines (31a,b) as crudes were pure enough and thus were not purified: IR 3050, 2950, 2800, 1740 cm^{-1}. Anal. Calcd for $C_{18}H_{28}N_2O_3Si$: C, 62.03; H, 8.10; N, 8.04. Found: C, 62.09; H, 8.07; N, 8.10.

(h) 3-Carbomethoxy-3-(1′-acetoxyethyl)-1-pyrazolines (32a,b) were purified by flash chromatography (hexanes/Et_2O = 3/7): IR 3000, 2900, 2800, 1740, 1570 cm^{-1}. Anal. Calcd for $C_9H_{14}N_2O_4$: C, 50.46; H, 6.59; N, 13.08. Found: C, 50.41; H, 6.63; N, 13.02.

(i) 3-Carbomethoxy-3-(1′-acetoxybutyl)-1-pyrazolines (33a,b) were purified by flash chromatography (hexanes/Et_2O = 4/6): IR 2950, 1750, 1650 cm^{-1}. Anal. Calcd for $C_{11}H_{18}N_2O_4$: C, 54.53; H, 7.49; N, 11.56. Found: C, 54.50; H, 7.51; N, 11.60.

(j) 3-Carbomethoxy-3-(1′-acetoxy-2′-methylpropyl)-1-pyrazolines (34a,b) were purified by flash chromatography (hexanes/Et_2O = 1/1): IR 2950, 1750, 1650, 1400 cm^{-1}. Anal. Calcd for $C_{11}H_{18}N_2O_4$: C, 54.56; H, 7.49; N, 11.57. Found: C, 54.50; H, 7.51; N, 11.60.

(k) 3-Carbomethoxy-3-[(1′-acetoxyphenyl)methyl]-1-pyrazolines (35a,b) were used without further purification: IR 3100, 3000, 2900, 1740, 1700 cm^{-1}. Anal. Calcd for $C_{14}H_{16}N_2O_4$: C, 60.86; H, 5.84; N, 10.14. Found: C, 60.90; H, 5.87; N, 10.09.

Chemical Correlation between 26a and 29a (Scheme 3). Compound **26a,b** (**a/b** mixture = 80/20) was silylated according to the procedure described for the synthesis of **5−8**. 1-Pyrazoline **29a,b** was obtained in 30% yield (**a/b** mixture = 80/20); unreacted starting material (**a/b** ratio = 80/20) and isomerized product **37a,b** (for its characterization, see below; **a/b** ratio = 80/20) were also isolated. Purification by flash chromatography was performed with a hexanes/Et_2O = 8/2 mixture as eluant.

Synthesis of 5-Carbomethoxy-5-[1′-[(*tert*-butyldimethylsilyl)oxy]butyl]-2-pyrazolines (37a,b) (Scheme 3). An 80/20 mixture of **29a,b** (1 mmol) was dissolved in CH_3CN (5 mL) and treated at 0 °C with 5 drops of 40% HF. The mixture was stirred for 8 h at room temperature, then neutralized with solid $NaHCO_3$, and filtered. Flash chromatography (hexanes/Et_2O = 7/3) allowed recovery of **37a,b** (72% yield, 80/20 mixture): IR 3400, 3000, 1750, 1680 cm^{-1}; ^1H and ^{13}C NMR data are collected in Table 4. Anal. Calcd for $C_{15}H_{30}N_2O_3Si$: C, 57.28; H, 9.62; N, 8.91. Found: C, 57.25; H, 9.60; N, 8.93.

Synthesis of 7-Carbomethoxy-2,8-di(propyl)-6*H*,7*H*-dihydropyrazo[2,3-*c*]-2*H*,3*H*,7*H*,8*H*-tetrahydroxazoles (36a,b) (Scheme 3). 26a or **26b** was separately treated with acetyl chloride according to the same procedure used for the synthesis of **9−12**; after 2 h at 0 °C, the reaction was quenched with diluted HCl. Flash chromatography (hexanes/Et_2O = 1/1) allowed recovery of **36a** and **36b**, respectively, in 30% yield, together with unreacted starting material: IR 2950, 1760, 1670 cm^{-1}; NMR data are collected in Table 5. Anal. Calcd for $C_{13}H_{22}N_2O_3$: C, 61.39; H, 8.72; N, 11.02. Found: C, 61.35; H, 8.74; N, 11.05.

Synthesis of 3-(Hydroxymethyl)-3-(1′-hydroxybutyl)-1-pyrazolines (38a,b) (Scheme 3). One millimole of **33a,b** (**a/b** ratio = 7/3) was dissolved in dry CH_2Cl_2 (10 mL) and treated at −78 °C with 6 molar equiv of DIBAL-H (1.5 M solution). After 3 h, a solution of NH_4Cl was added; the mixture was warmed to room temperature and filtered through a Celite pad, and then the residue was washed with CH_2Cl_2. Diols **38a,b** (**a/b** ratio = 7/3) were purified by flash chromatography (Et_2O/MeOH = 97/3; yield = 44%). The same procedure was applied to the reduction of pure **26a** with 4 molar equiv of DIBAL-H: pure **38a** was obtained, after purification, in 25% yield: NMR data are collected in Table 4; IR 3400, 3000, 2900, 2800, 2300 cm^{-1}. Anal. Calcd for $C_8H_{16}N_2O_2$: C, 55.79; H, 9.36; N, 16.27. Found: C, 55.74; H, 9.40; N, 16.23.

Synthesis of 3-(Hydroxymethyl)-3-[1′-[(*tert*-butyldimethylsilyl)oxy]butyl]-1-pyrazolines (39a,b) (Scheme 4). One millimole of **29a** (or **29b**) was dissolved in dry CH_2Cl_2 (10 mL) and treated at −78 °C with 3.5 molar equiv of DIBAL-H (1.5 M solution); after 30 min, the reaction was warmed to 0 °C in 2 h. A solution of NH_4Cl was added; the mixture was filtered through a Celite pad, and the residue was washed and extracted with CH_2Cl_2. Alcohols **39a** and **39b** were purified by flash chromatography (Et_2O/hexanes = 7/3; yield = 44%): IR 3450, 3000, 1650 cm^{-1}; NMR data are collected in Table 4. Anal. Calcd for $C_{14}H_{30}N_2O_2Si$: C, 58.69; H, 10.56; N, 9.78. Found: C, 58.72; H, 10.53; N, 9.76.

Synthesis of 5-[[(*tert*-butyldimethylsilyl)oxy]methyl]-5-(1′-hydroxybutyl)-2-pyrazoline (40a) (Scheme 4). 39a (1 mmol) was treated with 70% HF (2 drops) in CH_3CN or THF (3 mL) at 0 °C for 2 h; workup with solid $NaHCO_3$ allowed recovery of **40a** in 52% yield after flash chromatography (Et_2O/hexanes = 6/4): IR 3500, 2950, 1660 cm^{-1}; NMR data are collected in Table 4. Anal. Calcd for $C_{14}H_{30}N_2O_2Si$: C, 58.69; H, 10.56; N, 9.78. Found: C, 58.66; H, 10.58; N, 9.80.

Synthesis of 2,2-Dimethyl-7-[1′-[(*tert*-butyldimethylsilyl)oxy)butyl]-6*H*,7*H*-dihydropyrazo[2,3-*c*]-2*H*,3*H*,7*H*,8*H*-tetrahydroxazoles (41a,b) (Scheme 4). 39a or **39b** (0.2 mmol) was dissolved in 2,2-dimethoxypropane (2 mL) and MeOH (0.3 mL) and treated with 3 drops of 70% HF at 0 °C. The mixture was allowed to stand at room temperature for 2 h and then quenched with solid $NaHCO_3$. Flash chromatography (hexanes/Et_2O = 6/4) allowed recovery of pure **41a** and **41b**, respectively (66%): IR 3000, 1670 cm^{-1}; NMR data are collected in Table 5. Anal. Calcd for $C_{17}H_{34}N_2O_2Si$: C, 62.53; H, 10.49; N, 8.58. Found: C, 62.57; H, 10.47; N, 8.60.

NMR Experiments. 2D NOESY experiments were performed at 24 °C on 25 mM solutions of **36a** and **36b** previously degassed by several freeze−pump thaw cycles on a high-vacuum line to remove dissolved oxygen; 256 fids of 160 transients each were acquired with a mixing time of 1.4 s, a relaxation time of 5 s, and an acquisition time of 0.4 s. The data were apodized with a shifted sine-bell (90°) in both dimensions. The inverses quantum coherence experiments (HMQC and HMBC) were recorded on the instrument equipped with a 5 mm inverse broad band probe head without decoupling during acquisition using conventional Bruker software pulse sequences. The experimental conditions were as follows: 256 experiments of 128 scans each, relaxation delay 1 s, Δ = 3.54 and 60 ms (optimized for $^1J_{C,H}$ and $^nJ_{C,H}$, respectively; size 1 K; spectral width 2800 and 15 000 Hz in F_1 and F_2 respectively; sine-bell multiplication in both dimensions.

Computational Procedures. All geometry optimizations were performed with PM3[22] Hamiltonian using the package MOPAC 6.0.[23] Starting from the diazomethane plus ethylene transition structure,[6] the proper substituents were added and the transition structures optimized with a stepwise procedure. First, only the added substituents and subsequently all of the variables (excluding the two forming bonds and the C−C−O−H dihedral angle if fixed) were optimized using the PRECISE option. The transition structures were then fully optimized with the NLLSQ option (if the C−C−O−H dihedral angle was fixed at 180°) or with the TS option if no variables were fixed. The gradient was subsequently reduced with the GNORM=0.1 option, and then a FORCE calculation was performed to ensure the nature of the stationary points. All transition structures thus located presented only one imaginary frequency, corresponding to the symmetric stretch of the two forming bonds.

In the evaluation of the relative energies, the heat of formation values as calculated by the program were used. No evaluation of the entropic contribution to the activation energies was attempted, since we were interested in energy differences: we assumed that the entropic contribution is equal for each of the three different conformations of the same transition structure and then can be neglected since it eliminates while the difference is calculated.

Ground state geometries were directly optimized with the EF GNORM=0.1 options; the nature of the stationary points was established via a FORCE calculation. All PM3 calculations were run on a MicroVax 3100 or a VaxStation 3100 (Digital).

Acknowledgment. We gratefully acknowledge partial financial support from CNR-Piano Finalizzato Chimica Fine 2. We thank Giuseppina Intravaia and Carla Pasquarello for collaboration and Prof. I. E. Markò for helpful discussion.

JO941640L